

Depth-resolved analysis of ferroelectric domain structures in bulk LiNbO_3 crystals by scanning force microscopy

T. Jungk^{a)} and E. Soergel

Physical Institute, University of Bonn, Wegelerstraße 8, 53115 Bonn, Germany

(Received 11 March 2005; accepted 10 May 2005; published online 7 June 2005)

Ferroelectric domains were written in congruently melting lithium niobate crystals (LiNbO_3) by electrical field poling using a mask with circular openings. For the surface sensitive detection of the domains, we used scanning force microscopy. Thinning the crystal step-by-step reveals that the domains evolve from circular shape at the very surface to hexagonal shape at a depth of around $30\text{ }\mu\text{m}$, demonstrating the impact of the crystal symmetry on the domain shape. © 2005 American Institute of Physics. [DOI: 10.1063/1.1949286]

Domain engineering in lithium niobate crystals (LiNbO_3) has become important for photonics: Periodically-poled crystals facilitate nonlinear-optical applications, such as second-harmonic generation and optical parametric oscillation through quasi-phase matching.^{1,2} Tailored domain structures also allow to realize electro-optically tunable diffractive-optical elements.³ High-density data storage has been realized by writing and reading of nanodomains in ultrathin crystals.⁴ Arrays of inverted ferroelectric domains can also serve as nonlinear photonic crystals.⁵ These examples underline that the fabrication of μm -sized domain structures is a very active field.

Commonly, domain patterns are produced in bulk crystals using electric-field poling with structured electrodes.⁶ For the fabrication of periodically-poled crystals, the electric field is designed such that the stripes follow the crystallographic y axis. Due to the three-fold symmetry of the crystal, stripes and hexagons are the preferred domain shapes. Indeed, domains produced by arbitrarily shaped electrodes reshape into the crystallographically favored form while penetrating from the surface into the crystal volume.⁷ However, there is demand for micrometer-sized domain structures beyond the crystallographic constraints. Therefore, a study of the evolution of user-defined domain structures from the surface into the material depth is of relevance.

As an optimum tool for the nondestructive investigation of ferroelectric domains, scanning force microscopy (SFM) has been established⁸ because it allows one to reveal the domain structure at the very surface with a high lateral resolution. In this letter, we report depth-resolved mapping of ferroelectric domains using SFM.

A congruently melting, z -cut LiNbO_3 crystal (thickness $500\text{ }\mu\text{m}$, Crystal Technology, Inc.) was used for the experiments. For structured electric-field poling, the crystal was covered at the $-z$ face with a photoresist pattern to shape the electric field for selective domain inversion. The photoresist mask had circular openings with a diameter of $8\text{ }\mu\text{m}$ and the size of the structured area was about $10 \times 20\text{ mm}^2$. Both z faces were contacted homogeneously with gel electrodes and a voltage was applied to reverse the polarity of the sample at the openings of the photoresist mask. Figure 1 depicts schematically the resulting domains and introduces the nomenclature used later in the text.

To reveal the obtained domain structures both at the top and the bottom face of the crystal, we etched part of the sample in pure hydrofluoric acid (48%) for 15 min.⁹ This so-called differential etching identifies unequivocally the domain structure. To get information about the depth evolution of the domain shape, we subsequently thinned the sample by polishing the $-z$ face in steps of about $3\text{ }\mu\text{m}$ and took SFM images of the surface domain pattern after each step without etching. The step height was determined with a high precision caliper with an accuracy of about $1\text{ }\mu\text{m}$.

For the detection of the domain patterns, we utilized a commercial scanning force microscope (SMENA, NT-MDT), modified to allow application of voltages to the tip. We used stiff cantilevers (force constant $\approx 20\text{ N/m}$, resonance frequency $\approx 250\text{ kHz}$) with gold-coated tips and operated the instrument as a dynamic contact electrostatic force microscope (DC-EFM).¹⁰ The measurements were performed in contact mode with an additional ac voltage (10 V , 36 kHz) applied to the tip. Even though the tip is in contact with the surface, the cantilever vibrates at the applied frequency due to the electrostatic interaction of the periodically charged tip with the field of the domains. The time constant of the feedback circuit being very large compared to the inverse of the modulation frequency of the voltage applied to the tip, the topography can be read out as in standard contact mode SFM. From the modulated electrostatic force signal, we get information about the domain structure of our sample via lock-in detection.¹¹ The phase of the lock-in amplifier is adjusted such that $+z$ ($-z$) faces appear as dark (bright) areas in the images. The lateral resolution for the domain contrast images is $\approx 200\text{ nm}$. Topography and domain structure of the sample surface can be read out simultaneously.

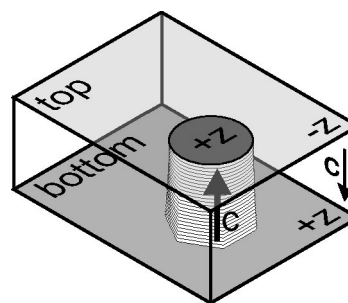


FIG. 1. Schematic view of the LiNbO_3 sample and its domain structure.

^{a)}Electronic mail: jungk@physik.uni-bonn.de

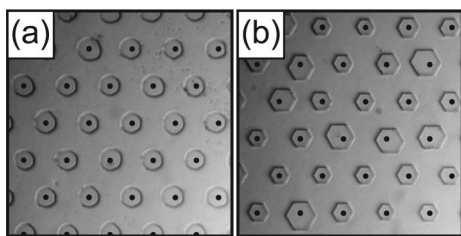


FIG. 2. Optical microscope images ($100 \times 100 \mu\text{m}^2$) of both faces of the etched LiNbO₃ crystal with circles at the top (a) and hexagons at the bottom surface (b). The dots indicate the lattice of the photoresist mask.

In the first experiment, we investigated the part of the LiNbO₃ crystal that was etched in hydrofluoric acid, therefore revealing unambiguously the domain structures. Figure 2 shows optical microscopic images of both crystal faces after etching. The figure clearly displays circular domains at the top surface [Fig. 2(a)] and hexagonal domains at the bottom [Fig. 2(b)]. The same domain patterns can also be seen on the nonetched part of the crystal with DC-EFM (Fig. 3). Note that the dots are dark and the hexagons are bright because we have to flip the crystal for scanning the bottom face, therefore inverting the contrast of the domain pattern. The domains appear longish because of the nonlinearity of the piezoscanner.

From these pictures, we can figure out the size distribution of the areas with reversed polarization on the structured $-z$ face and on the homogeneously gel-covered $+z$ face of the crystal. Whereas the circles are rather uniform with a diameter of 8 to 9 μm , the size of the hexagons scatters roughly by a factor of 2 from 6 to 13 μm . Indeed, the hexagons are also generally regular.

Domains becoming larger in electric-field poling along their way through the crystal is known as domain spreading;¹² one of the main challenges for μm -sized domain engineering. This effect is explained via the field enhancement at the edges of the photoresist pattern and should lead to a symmetric broadening of the inverted areas. But by comparing the centers of the hexagonal domains with the regularly spaced array of black dots that are superimposed on the image in Fig. 2(b), it is obvious that the large hexagons are arbitrarily misaligned. Note that the circular domains are nearly perfectly arranged [Fig. 2(a)]. We therefore expect that crystal defects influence the poling properties are the primary cause for these irregularities.

Domains shrinking on their way through the crystal presume that the poling process was aborted too early. However, the total domain inverted area, as it is determined from large

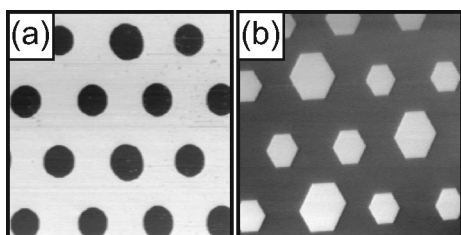


FIG. 3. DC-EFM images of the top (a) and the bottom (b) surface of the nonetched LiNbO₃ crystal. The image size is $60 \times 60 \mu\text{m}^2$. In our settings the $-z/+z$ faces show up as bright/dark areas, hence the contrast of the written domains seems inverted—locking once from the top and once from the bottom. The domains seem long because of the nonlinearity of the piezoscanner. The topography (not shown) exhibits no particularities.

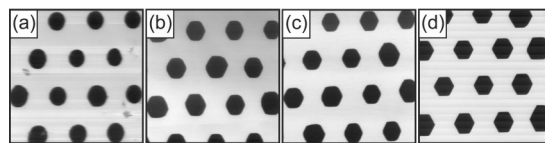


FIG. 4. DC-EFM images of the top surface of the nonetched LiNbO₃ crystal. The image size is $60 \times 60 \mu\text{m}^2$. The images are taken after polishing to a depth of 8 μm (a), 17 μm (b), 26 μm (c), and 35 μm (d) below the original surface of the crystal.

images (0.25 mm^2), is 21% for both crystal faces. Since domain reversal does not start simultaneously for all sites, some domains have grown larger than desired whereas others have not yet reached their required size. Note that the small hexagons are mainly centered with respect to the superimposed dot array. The domains therefore seem to reach the bottom face of the crystal as hexagons centered to the photoresist openings, and asymmetric sideways growing occurs later.

In further experiments, we examined the transition from the circular shape of the domains at the top surface to their hexagonal shape at the bottom. Figure 4 shows a selection of the series of images that we got from successively thinning the crystal and imaging the resulting domain structure with the SFM. Whereas at a depth of 8 μm [Fig. 4(a)], the domains are still circular the orientation of the crystal can already be anticipated at 17 μm [Fig. 4(b)]. Deeper inside the crystal, 26 μm below the surface [Fig. 4(c)] hexagons with rounded edges can be seen, and at 35 μm [Fig. 4(d)] the domains show a very clear hexagonal shape. However, at this depth, the size distribution of the hexagons is rather uniform: They vary from 9 to 10 μm . This results in the same domain inverted area as for the circles whose size is about 8 to 9 μm in diameter. The center of these hexagons, 35 μm below the original surface, also matches the lattice of the photoresist pattern.

Comparing Fig. 4(d) (at a depth of 35 μm) with Fig. 3(b) (back side of the crystal corresponding to a depth of 500 μm), it turns out that on their way through the crystal, the hexagons are altered even further: Some get smaller whereas others grow, and the center of the large ones is displaced. Although they have achieved their preferred hexagonal geometry at a depth of 35 μm , where the high-field gradients from the edges of the photoresist that caused domain spreading are no longer dominant, they still vary with respect to their size.

To get information about the stability of the domains, we have annealed the crystal for 24 h at 400 $^{\circ}\text{C}$ to release all internal stress,¹³ however, the domain structures were not affected. Also noteworthy is that the polishing procedure did not influence the domain shape. The circularly shaped domains are thus stable enough for applications.

One might think that a single experiment would reveal the evolution of the shape by directly measuring the topography of the domain pillows of a deeply etched sample with the SFM or a scanning electron microscope. This is, however, not accurate because etching also affects the x and y faces of the crystal.⁷ Therefore, no clear information about the shape of the domains could be gathered from such an experiment.

In this letter, we have demonstrated a precise and simple method for the depth-resolved analysis of ferroelectric domains. We have shown that the maximum depth at which

arbitrary domain patterns can be imposed into a congruently melting LiNbO_3 crystal by structured external electrical fields is about $10\ \mu\text{m}$, if there is no match between the structure and the preferred crystallographic axes.

The authors are grateful to C. Gawith from the Optoelectronics Research Centre, Southampton, for the preparation of the sample and to R. W. Eason, S. Mailis, and K. Buse for fruitful discussions. Financial support of the DFG Research Unit 557 and of the Deutsche Telekom AG is gratefully acknowledged.

¹L. E. Myers, G. D. Miller, R. C. Eckardt, M. M. Fejer, R. L. Byer, and W. R. Bosenberg, *Opt. Lett.* **20**, 52 (1995).

²M. M. Fejer, G. A. Magel, D. H. Jundt, and R. L. Byer, *IEEE J. Quantum Electron.* **28**, 2631 (1992).

³M. Yamada, *Rev. Sci. Instrum.* **71**, 4010 (2000).

⁴Y. Cho, K. Fujimoto, Y. Hiranaga, Y. Wagatsuma, A. Onoe, K. Terabe, and K. Kitamura, *Appl. Phys. Lett.* **81**, 4401 (2002).

⁵N. G. R. Broderick, G. W. Ross, H. L. Offerhaus, D. J. Richardson, and D. C. Hanna, *Phys. Rev. Lett.* **84**, 4345 (2000).

⁶M. Yamada, N. Nada, M. Saitoh, and K. Watanabe, *Appl. Phys. Lett.* **62**, 435 (1993).

⁷I. E. Barry, G. W. Ross, P. G. R. Smith, R. W. Eason, and G. Cook, *Mater. Lett.* **37**, 246-254 (1998).

⁸P. Güthner and K. Dransfeld, *Appl. Phys. Lett.* **61**, 1137 (1992).

⁹C. L. Sones, S. Mailis, W. S. Brocklesby, R. W. Eason, and J. R. Owen, *J. Mater. Chem.* **12**, 295 (2002).

¹⁰J. W. Hong, K. H. Noh, S. Park, S. I. Kwun, and Z. G. Khim, *Phys. Rev. B* **58**, 5078 (1998).

¹¹M. Labardi, V. Likodimos, and M. Allegrini, *Phys. Rev. B* **61**, 14390 (2000).

¹²V. Y. Shur, E. L. Rumyantsev, E. V. Nikolaeva, E. I. Shishkin, D. V. Fursov, R. G. Batchko, L. A. Eyres, M. M. Fejer, and R. L. Byer, *Appl. Phys. Lett.* **76**, 143 (2000).

¹³V. Gopalan and M. C. Gupta, *J. Appl. Phys.* **80**, 6099 (1996).